

# Induced transparency in optomechanically coupled resonators

Zhenglu Duan<sup>1</sup>, Bixuan Fan<sup>1</sup>, Thomas M. Stace<sup>2</sup>, G. J. Milburn<sup>2</sup> and Catherine A. Holmes<sup>3\*</sup>

<sup>1</sup>College of Physics, Communication and Electronics,  
Jiangxi Normal University, Nanchang, 330022, China

<sup>2</sup>Center for Engineered Quantum Systems, School of Mathematics and Physics,  
The University of Queensland, St Lucia, Queensland 4072, Australia and

<sup>3</sup>School of Mathematics and Physics, University of Queensland, St Lucia, 4072, Qld, Australia

In this work we theoretically investigate a hybrid system of two optomechanically coupled resonators, which exhibits induced transparency. This is realized by coupling an optical ring resonator to a toroid. In the semiclassical analyses, the system displays bistabilities, isolated branches (isolas) and self-sustained oscillation dynamics. Furthermore, we find that the induced transparency transparency window sensitively relies on the mechanical motion. Based on this fact, we show that the described system can be used as a weak force detector and the optimal sensitivity can beat the standard quantum limit without using feedback control or squeezing under available experimental conditions.

PACS numbers: 42.65.Pc, 42.50.Wk, 42.50.Nn, 07.07.Df

*Introduction.* The coupled-resonator induced transparency (CRIT), arising when light passes through two closely located identical ring optical resonators, was first put forward in [1] and then experimentally observed in [2, 3]. This transparency comes from the interference between two pathways of the light, leading to the Fano effect in the coupled ring resonator system. The CRIT effect has a wide variety of applications in linear regime, such as slowing and stopping light [4, 5], signal routing [6], and biomedical molecule sensing [7]. In the highly nonlinear regime, the system shows bistability [8], which can be used for optical switching [9].

Here we consider such a situation: One of the ring resonators in CRIT is replaced by an optomechanical system (toroidal), in which the optical mode and mechanical vibration mode are coupled through radiation pressure coupling. This simple structure forms a hybrid CRIT and optomechanical system. As we show the interplay between CRIT and optomechanics can lead to more interesting effects. In particular by including the optomechanical nonlinearity the transparency window of the CRIT becomes tunable and also exhibits bistability. In addition the coupled system undergoes saddle node and Hopf bifurcations which result in the emergence of bistabilities, isolated branches (isolas) [10, 11] and self-sustained oscillations.

Detection of weak forces with high sensitivity has long been a research focus. Optomechanical systems are ideal for detecting small perturbations including weak forces [12–15]. The general idea for realizing those proposals is to map a weak force onto the shift in position of a mechanical system that can be easily monitored by the coupled optical field. Also, precise quantum measurements can be performed via monitoring transparency windows

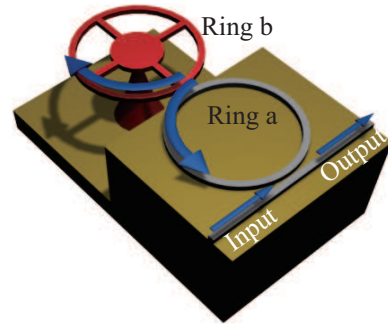


FIG. 1: (Color online) Schematic for the coupled-resonator system with optomechanical coupling. An optical ring resonator (the green ring) is coupled to a toroid (the red ring) evanescently. In the toroid, the optical mode and mechanical mode interact through radiation pressure.

in EIT or its analog, the optomechanically induced transparency (OMIT) [16–18], for instance, measurements of magnetic fields [19, 20], Rydberg states [21], number of electric charges [22] and transition dipole moments [23]. Stimulated by these possible applications we utilize the large dispersion of the CRIT transparency window and the sensitive dependence of CRIT on mechanical motion to detect a weak force applied on the mechanical mode. With shot noise and environmental thermal noise included, we estimate that the optimal force sensitivity is  $17\text{aN}\cdot\text{Hz}^{-1/2}$  when the system operates at resonance.

*Model.* The system under consideration is shown in figure 1: a ring optical resonator is evanescently coupled to a toroidal optomechanical system and a driving field is applied on the optical resonator through a waveguide. In the frame rotating at the driving field frequency  $\omega_{\text{in}}$ , we write down the equations of motion for the system

[1] \*Corresponding author, cah@maths.uq.edu.au

operators:

$$\dot{\hat{x}} = \omega_m \hat{p} \quad (1)$$

$$\dot{\hat{p}} = -\gamma_m \hat{p} - \omega_m \hat{x} + g_1 \hat{b}^\dagger \hat{b} + \hat{\xi}_m \quad (2)$$

$$\dot{\hat{a}} = -(i\Delta + \kappa) \hat{a} - ig_2 \hat{b} + \hat{a}_{\text{in}} \quad (3)$$

$$\dot{\hat{b}} = -(i(\Delta + \delta - g_1 \hat{x}) + \kappa_b/2) \hat{b} - ig_2 \hat{a} + \sqrt{\kappa_b} \hat{b}_{\text{vac}} \quad (4)$$

where  $\hat{x}$  and  $\hat{p}$  are the dimensionless position and momentum operators for the mechanical degree of freedom with frequency  $\omega_m$ .  $\hat{a}$  and  $\hat{b}$  are annihilation operators of the optical modes in the resonator and toroid, with frequencies  $\omega_a$  and  $\omega_b$  and damping rates  $\kappa_a$  and  $\kappa_b$ .  $\kappa = (\kappa_a + \kappa_{\text{ex}})/2$ .  $\Delta = \omega_a - \omega_{\text{in}}$  is the detuning between the driving light and the optical resonator  $\hat{a}$  and  $\delta = \omega_b - \omega_a$  is the frequency difference between two optical modes.  $g_1$  is the optomechanical coupling coefficient between the optical mode  $\hat{b}$  and the mechanical mode of the toroid and  $g_2$  is the coupling coefficient between two optical modes.  $\kappa_{\text{ex}}$  is the outgoing coupling coefficient from the optical resonator into the waveguide.  $\hat{a}_{\text{in}} = \sqrt{\kappa_{\text{ex}}}(\sqrt{I_{\text{in}}} + \delta \hat{a}_{\text{in}}) + \sqrt{\kappa_a} \hat{a}_{\text{vac}}$  where the driving light intensity  $I_{\text{in}}$  with fluctuation  $\delta \hat{a}_{\text{in}}$ .  $\hat{a}_{\text{vac}}$  and  $\hat{b}_{\text{vac}}$  are the external vacuum fields to optical modes a and b, respectively. The mechanical mode is affected by a viscous force with the damping rate  $\gamma_m$  and by a Brownian stochastic force with noise  $\hat{\xi}_m$ .

When the system is strongly driven, it can be characterized by the semiclassical steady-state solutions with large amplitudes for both mechanical and optical modes. In the following, we denote  $y_s$  as the steady-state mean value of the operator  $\hat{y}$ . By setting the time derivatives of system variables to zero and factorizing the expectation values, the steady-state solutions are obtained:

$$x_s = \frac{g_1 g_2^2 |a_s|^2}{\omega_m (\Delta_{\text{eff}}^2 + \kappa_b^2/4)} \quad (5)$$

$$a_s = \frac{\sqrt{\kappa_{\text{ex}}} I_{\text{in}}}{(i\Delta + \kappa + g_2^2/(i\Delta_{\text{eff}} + \kappa_b/2))} \quad (6)$$

$$b_s = -\frac{ig_2}{(i\Delta_{\text{eff}} + \kappa_b/2)} a_s \quad (7)$$

with the effective detuning  $\Delta_{\text{eff}} = \Delta + \delta - g_1 x_s$ . Eq. (5) is a cubic equation for the steady state value  $x_s$ , therefore there are at most three real roots.

Next, we turn to study fluctuations around the steady state by expanding the system operators around their stable-state values, i.e.,  $\hat{y} \rightarrow y_s + \hat{y}$ , and introducing the field quadrature fluctuations  $\hat{X}_c = (\hat{c} + \hat{c}^\dagger)/\sqrt{2}$  and  $\hat{Y}_c = (\hat{c} - \hat{c}^\dagger)/(\sqrt{2}i)$  ( $\hat{c} = \hat{a}, \hat{b}, \hat{a}_{\text{in}}, \hat{a}_{\text{vac}}, \hat{b}_{\text{vac}}$ ). Ignoring high-order terms of fluctuations, the linearized equations of motion can be written as  $\dot{\hat{y}} = J\hat{y} + \xi$  where  $\hat{y} = [\hat{x}, \hat{p}, \hat{X}_a, \hat{Y}_a, \hat{X}_b, \hat{Y}_b]^T$ , the noise term  $\xi = [0, \hat{\xi}_m, \sqrt{\kappa_{\text{ex}}}\hat{X}_{\text{in}} + \sqrt{\kappa_a}\hat{X}_{\text{vac}}, \sqrt{\kappa_{\text{ex}}}\hat{Y}_{\text{in}} + \sqrt{\kappa_a}\hat{Y}_{\text{vac}},$

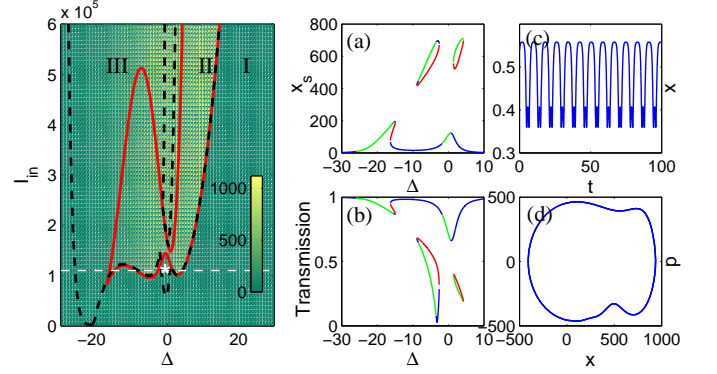


FIG. 2: (Color online) Left panel: The bifurcation diagram for the position of the mechanical resonator in the  $(\Delta, I_{\text{in}})$  plane. The red solid curve labels the boundary of saddle-node bifurcations and the black dashed curve labels the boundary of Hopf bifurcations. The stable region is denoted by region I, which is the area outside of red and black curves. The area within the red curve is region II, in which multiple steady states exist. Region III, enclosed with black curve, is the parametric unstable region, with self sustained oscillations created in the Hopf bifurcation. In right panel, figure (a) is a cross section of left panel labeled by the white dashed line. The blue, red and green curves denote stable, unstable and parametric unstable solutions. Figure 2 (b) shows the corresponding light transmission of (a). The parameters are  $k_a = 0.6$ ,  $k_b = 4.0$ ,  $k_{\text{ex}} = 4$ ,  $\delta = 20$ ,  $g_1 = 0.03$ ,  $g_2 = 4$ ,  $\omega_m = 1$  and  $\gamma_m = 0.1$ . Figures 2 (c) and (d) present the dynamics and its corresponding phase space picture for one point in region III  $(\Delta, I_{\text{in}}) = (-0.25, 1.1 \times 10^5)$ , as labelled using a white star in the left panel.

$\sqrt{\kappa_b}\hat{X}_{\text{vac}}, \sqrt{\kappa_b}\hat{Y}_{\text{vac}}]^T$ , and the Jacobian matrix is given by

$$J = \begin{pmatrix} 0 & \omega_m & 0 & 0 & 0 & 0 \\ -\omega_m & -\gamma_m & 0 & 0 & g_1 X_{bs} & g_1 Y_{bs} \\ 0 & 0 & -\kappa & \Delta & 0 & g_2 \\ 0 & 0 & -\Delta & -\kappa & -g_2 & 0 \\ -g_1 Y_{bs} & 0 & 0 & g_2 & -\kappa_b/2 & \Delta_{\text{eff}} \\ g_1 X_{bs} & 0 & -g_2 & 0 & -\Delta_{\text{eff}} & -\kappa_b/2 \end{pmatrix}, \quad (8)$$

where  $X_{bs} = (b_s + b_s^*)/\sqrt{2}$ , and  $Y_{bs} = (b_s - b_s^*)/(\sqrt{2}i)$ . The steady-state solution is stable if all eigenvalues of the Jacobian matrix have negative real parts. The Routh-Hurwitz criterion [24] can be used to determine the stable and unstable regions in the parameter space.

To illustrate the stability of the described system, the phase diagram for the mechanical position of the toroid in the parameter space  $(\Delta, I_{\text{in}})$  is pictured in left panel of figure 2. The whole plane is divided into stable, unstable and parametric unstable regions, which are divided by saddle-node bifurcations (red solid curve) and Hopf bifurcations (black dashed curve). In particular, we plot a cross section of the left figure in figure 2 (a) as labeled by the typical bistable branch on the main continuous

curve and two isolated branches (isolas) above the lower main branch. Supposing that initially the equilibrium position of the mechanical resonator is on an isolated branch, if the detuning  $\Delta$  is continuously swept in an increasing or decreasing manner, the equilibrium position will jump to the lower main branch, but not vice versa. This unique feature is a non-hysteretic bistability, which can be used as a unidirectional switch. In fact, the stability of the isolas are similar to conventional S-type bistabilities in the higher-dimensional parameter space. In experiments the light transmission  $T \equiv |a_{\text{out}}/\sqrt{I_{\text{in}}}|^2$  is more directly observable. According to the input-output relation  $a_{\text{out}} = \sqrt{I_{\text{in}}} - \sqrt{\kappa_{\text{ex}}}a_s$ , the light transmission can be related to the mechanical position as

$$T = \left| 1 - \sqrt{\kappa_{\text{ex}}/I_{\text{in}}}a_s \right|^2 \quad (9)$$

Figure 2 (b) presents the equilibrium curve of the light transmission corresponding to figure 2(a) and one can observe that it also shows hysteretic behaviors and the emergence of isolas.

The presence of the parametric unstable region comes from the choosing parameters lying in unresolved side-band regime with small mechanical damping, i.e.,  $1 > \omega_m/\kappa_b > \gamma_m$ . Figure 2(c) presents the same in the parametric unstable region (III) where the mechanics exhibits stable oscillatory motion. The corresponding phase space picture is displayed in figure 2(d) and one can easily find a stable closed phase trajectory ( a stable limit cycle).

*CRIT-like effect.* If the optomechanical coupling is switched off, the model reduces to a typical optical coupled-resonator system, which manifests the CRIT effect for certain parameters [1, 25]. In the following we investigate how the nonlinearity induced by the mechanical resonator changes the CRIT effect. For simplicity, we consider two optical resonators with the same frequency, i.e.,  $\delta = 0$ , the vanishing decay of the optical field in the toroid, low driving intensity and  $\kappa_a = \kappa_{\text{ex}}$ . Under these assumptions, Eq. (9) becomes

$$T = \left[ 1 + \kappa^2 / (\Delta - g_2^2 / (\Delta - g_1 x_s))^2 \right]^{-1} \quad (10)$$

which is a CRIT-like function with the transparency window width  $g_2$  and the center position of the transparency window located at  $g_1 x_s$ . Recall that  $x_s$  is dependent on the detuning  $\Delta$  and the input light intensity  $I_{\text{in}}$ . Eq. (10) shows us how the presence of the mechanical motion modifies the behaviors of CRIT.

In figures 3(a)-(d), the transmission  $T$  is plotted versus the detuning  $\Delta$  with different input light intensities. It is seen that, for a small driving intensity, there is a symmetric narrow transparency window in the middle of transmission spectrum (figure 3(a)), which is very similar to the typical CRIT effect except for a slight shift of the center of the transparency window. The result can be explained as follows, for a tiny input intensity, the value of

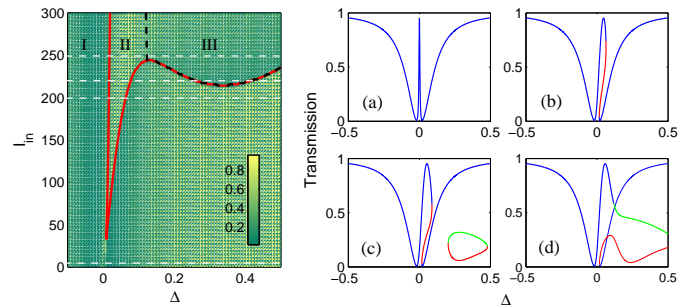


FIG. 3: (Color online) Left panel: the bifurcation diagram for the position of the mechanical resonator in the  $(\Delta, I_{\text{in}})$  plane. Right panel: the transmission as a function of detuning  $\Delta$  with different input light intensity. (a)  $I_{\text{in}} = 1$ , (b)  $I_{\text{in}} = 200$ , (c)  $I_{\text{in}} = 230$  and (d)  $I_{\text{in}} = 250$ , indicated by the white dashed lines in left panel. The parameters are  $\kappa_a = 0.1$ ,  $\kappa_b = 0.0002$ ,  $\kappa_{\text{ex}} = 0.1$ ,  $\delta = 0$ ,  $g_1 = 0.001$ ,  $g_2 = 0.02$ ,  $\omega_m = 1$  and  $\gamma_m = 0.001$ .

the mechanical resonator position can be approximately rewritten as

$$x_{s0} = g_1 \kappa_{\text{ex}} I_{\text{in}} / (\omega_m g_2^2) \quad (11)$$

which is independent of  $\Delta$ . Therefore the mechanical motion merely shifts the center without changing the shape of the transparency window. With  $I_{\text{in}}$  increasing, the transparency window bends towards the right side and the transmission curve becomes bistable (figure 3(b)). It is interesting that, for certain  $I_{\text{in}}$ , the distorted transparency window breaks into a mother branch and an isola (figure 3(c)). With further increasing  $I_{\text{in}}$ , the transparency window becomes severely distorted, even intersecting with itself and forming a closed loop (figure 3(d)). From Eqs. (4) and (5) we can understand this phenomenon by noting that the steady-state position of the mechanical resonator shifts to right-hand side in a way that depends on the detuning for large  $I_{\text{in}}$  (shown in the left panel of figure 3). For large enough input light intensity, the nonlinear shift causes an instability in intracavity photon number and system variables. These effects are dramatically different from the original CRIT effect, in which the transparency window is totally independent of the input light intensity and the shape is always symmetric.

*Weak force detection.* It is well known that, near transparency windows of EIT or similar effects like CRIT and OMIT, the dispersion is very large in the vicinity of the non-absorptive resonance point. Thus, a small detuning from the resonance will lead to a huge phase shift, which can be used for sensing small perturbations, for instance, ultra-sensitive detection of magnetic field [19, 20]. Here we utilize the CRIT effect and its dependence on optomechanical nonlinearity to design a weak force detector.

Assuming that an external force  $f$  is applied on the toroidal optomechanical system in our model and remem-

bering that  $\kappa_{\text{ex}}g_1x_s \ll g_2^2$ , we evaluate the new steady-state mechanical position involving the external force  $f$  as

$$x_s = \omega_m^{-1}f + x_{s0} \quad (12)$$

The external force shifts the steady-state position of mechanical resonator from  $x_{s0}$  to  $x_s$ , and thereby shifts the resonance of CRIT (see the dispersion spectrum in figure 4(b)). With appropriate parameters chosen, the slope of the dispersion curve in the vicinity of the resonance is huge. A weak external force can lead to a large phase shift along with small absorption of the input field, with an interferometric method, as shown in figure 4(a). This is the key idea of our proposal for weak force detection.

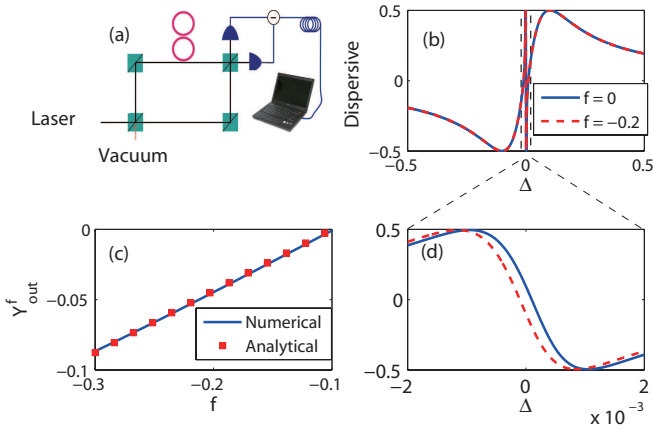


FIG. 4: (Color online) (a) The scheme for weak force detection by measuring phase shifts when a light passing through the hybrid CRIT-optomechanical system. (b) The dispersion of the system as a function of detuning  $\Delta$  with (red dashed line) and without (blue solid blue line) external forces. Figure (d) is the zooming in of the labeled region of figure (b). (c) The phase shift as a function of the external force  $f$ . The blue solid line presents the numerical result and the red dashed line is the approximate analytical result based on Eq. (13). The parameters are  $\kappa_a = 0.1$ ,  $\kappa_b = 0.00002$ ,  $\kappa_{\text{ex}} = 0.1$ ,  $\delta = 0$ ,  $\Delta = 0$ ,  $g_1 = 0.001$ ,  $g_2 = 0.01$ ,  $I_{\text{in}} = 0.1$ ,  $\omega_m = 1$  and  $\gamma_m = 0.1$ .

In figure 4(c) the solid curve represents the relation between the phase quadrature of the output field  $Y_{\text{out}}^f$  and  $f$ . One can see that, in the range of the plot, the phase quadrature linearly depends on  $f$ , which is ideal for measurements in practice. To analytically verify this conclusion, we find that, given the steady-state value of the mechanical resonator position very tiny, the phase quadrature can be approximated as

$$Y_{\text{out}}^f = \frac{\sqrt{2I_{\text{in}}\kappa_{\text{ex}}g_1}}{\omega_m g_2^2} (f + \omega_m x_{s0}). \quad (13)$$

From figure 4(c), it is clear that the approximate analytical result (13) well agrees with the numerical one.

Now we estimate the sensitivity of our force detection proposal. When the hybrid CRIT-optomechanics system operates at the resonant point, we transform the linearized quantum Langevin equations of motion to the frequency domain (see the supplementary material). According to the input-output relation, the phase quadrature of the output field in the homodyne detection can be presented as  $Y_{\text{out}}(\omega) = Y_{\text{in}}(\omega) - \sqrt{\kappa_{\text{ex}}}Y_a(\omega)$ . To calculate the sensitivity to the external force  $f$ , we define an effective force noise:

$$F(\omega) = \frac{Y_{\text{out}}(\omega)}{\partial Y_{\text{out}}(\omega)/\partial f} \Big|_{f=0}. \quad (14)$$

The total power spectral density of the effective force in the homodyne measurement of the phase quadrature is

$$\begin{aligned} S_{\text{FF}} &= \int d\omega' \langle F(\omega) F(\omega') \rangle \\ &= S_{\text{FF}}^{\text{th}} + S_{\text{FF}}^{\text{shot}} \end{aligned} \quad (15)$$

where the thermal noise spectral density is  $S_{\text{FF}}^{\text{th}} = 2m\gamma_m K_B T_R$  and the dimensional optical shot noise spectral density, for a Dc ( $\omega = 0$ ) force, is given by

$$S_{\text{FF}}^{\text{shot}}(0) \simeq \frac{\hbar m \omega_m^2}{4} \left[ \frac{1}{2} \frac{g_2^6}{(\kappa g_1 x_s)^3} - \frac{g_2^2}{(\kappa g_1 x_s)} + \frac{9}{2} \frac{(\kappa g_1 x_s)}{g_2^2} \right] \quad (16)$$

Here we have assumed  $\kappa_a, \kappa_b \ll \kappa_{\text{ex}}, g_2$ . The power spectral density or the square of the force sensitivity is minimized at  $g_2^2 \simeq 1.45\kappa g_1 x_s$ :

$$\min[S_{\text{FF}}^{\text{shot}}] \simeq 0.8\hbar m \omega_m^2 \quad (17)$$

This is below the standard quantum limit. Reasonable system parameters are assumed as:  $\omega_m \sim 20$  MHz,  $m \sim 9$  pg,  $\gamma_m \sim 40$  Hz,  $g_1 \sim 3$  MHz $\cdot$ nm $^{-1}$ ,  $g_2 \sim 4.6$  MHz,  $\kappa_1 \sim 1$  MHz,  $\kappa_2 \sim 0.01$  MHz,  $\kappa_{\text{ex}} \sim 200$  MHz, the optimal input power  $I_{\text{in}} \sim 10$   $\mu$ W. Using these parameters, the estimated optimal force sensitivity is  $\sqrt{S_{\text{FF}}^{\text{shot}}} \sim 17$  aN $\cdot$ Hz $^{-1/2}$  within 1s averaging time. This result is comparable to the experimental result reported in [15] but with shorter averaging time and without using feedback control.

*Conclusions.* We have investigated a CRIT system with one of the optical ring resonators replaced by a toroidal optomechanical resonator. The bistability of the light transmission and the equilibrium position of mechanical resonator were studied in the semiclassical limit. Interestingly, there are isolas and self-sustained oscillation dynamics appearing in the system. The nonlinearity induced by the optomechanical resonator on the CRIT effect was also studied. The result shows that the transparency window is dramatically affected by the optomechanical coupling. Finally, we suggested a weak force detection scheme based on the described system and found

that the optimal force sensitivity of  $17 \text{ aN}\cdot\text{Hz}^{-1/2}$  with available experimental conditions could be achieved.

Z.D. and B.F. acknowledge support from National Natural Science Foundation of China through Grant No. 11364021, No. 11504145 and No. 61368001, and Natural Science Foundation of Jiangxi Province through Grant No. 20122BAB212005.

## APPENDIX

In this appendix we give the detailed calculation for evaluating the force detection sensitivity.

The linearized equations of motion for the system variables in the frequency domain are given by

$$x = \chi_m \left[ \xi_m + f + \sqrt{2}\hbar g_1 b_s X_b \right] \quad (18)$$

$$(\kappa - i\omega) X_a = g_2 Y_b + \sqrt{\kappa_{\text{ex}}} X_d + \sqrt{\kappa_a} X_{\text{ac}} \quad (19)$$

$$(\kappa - i\omega) Y_a = -g_2 X_b + \sqrt{\kappa_{\text{ex}}} Y_d + \sqrt{\kappa_a} Y_{\text{ac}} \quad (20)$$

$$\left(\frac{\kappa_b}{2} - i\omega\right) X_b = -g_1 x_s Y_b + g_2 Y_a + \sqrt{\kappa_b} X_{\text{bc}} \quad (21)$$

$$\begin{aligned} \left(\frac{\kappa_b}{2} - i\omega\right) Y_b &= g_1 x_s X_b + \sqrt{2}g_1 b_s x - g_2 X_a \quad (22) \\ &+ \sqrt{\kappa_b} Y_{\text{bc}} \end{aligned}$$

where  $\chi_m^{-1} = m(\omega_m^2 - \omega^2 - i\gamma_m\omega)$  is the mechanical susceptibility. For simplicity we choose the initial condition of the system such that the phase of the optical field  $b$  is zero, i.e.,  $b_s$  is real.

According to the input-output relation, the phase quadrature of the output field is  $Y_{\text{out}} = Y_d - \sqrt{\kappa_{\text{ex}}} Y_a$ . After some calculation we arrive at

$$\begin{aligned} Y_{\text{out}} &= \frac{\chi_b g_2 \sqrt{\kappa_{\text{ex}}}}{(\kappa - i\omega)} (\chi_F (\xi_m + f) + \chi_{X_d} X_d) \quad (23) \\ &+ \chi_{X_{\text{ac}}} X_{\text{ac}} + \chi_{Y_{\text{bc}}} Y_{\text{bc}} + \chi_{Y_d} Y_d + \chi_{Y_{\text{ac}}} Y_{\text{ac}} + \chi_{X_{\text{bc}}} X_{\text{bc}} \end{aligned}$$

where

$$\chi_F = -\sqrt{2}\chi_m g_1 x_s g_1 b_s (\kappa - i\omega)^2 \quad (24)$$

$$\chi_{X_d} = g_1 g_2 x_s \sqrt{\kappa_{\text{ex}}} (\kappa - i\omega) \quad (25)$$

$$\chi_{Y_d} = \sqrt{\kappa_{\text{ex}}} \left( A g_2 + \frac{(\kappa - \kappa_{\text{ex}} - i\omega)}{\chi_b g_2 \kappa_{\text{ex}}} \right) \quad (26)$$

$$\chi_{X_{\text{ac}}} = g_1 g_2 x_s \sqrt{\kappa_a} (\kappa - i\omega) \quad (27)$$

$$\chi_{Y_{\text{ac}}} = \sqrt{\kappa_a} \left( A g_2 - \frac{1}{g_2 \chi_b} \right) \quad (28)$$

$$\chi_{X_{\text{bc}}} = A \sqrt{\kappa_b} (\kappa - i\omega) \quad (29)$$

$$\chi_{Y_{\text{bc}}} = -g_1 x_s \sqrt{\kappa_b} (\kappa - i\omega)^2 \quad (30)$$

and

$$A = (\kappa_b/2 - i\omega)(\kappa - i\omega) + g_2^2 \quad (31)$$

$$\chi_b^{-1} = A^2 + (g_1 x_s)^2 (\kappa - i\omega)^2 (1 + 2m\omega_m^2 \chi_m) \quad (32)$$

where  $\xi_m$  obeys the correlation  $\langle \xi_m(t) \xi_m(t') \rangle = 2m\gamma_m K_B T_R \delta(t - t')$  with Boltzmann constant  $K_B$  and

the environment temperature  $T_R$ . To calculate the sensitivity of force detection, an effective force noise is defined as

$$\begin{aligned} F(\omega) &= \left. \frac{Y_{\text{out}}(\omega)}{\partial Y_{\text{out}}(\omega) / \partial f} \right|_{f=0} \quad (33) \\ &= \xi_m + (\chi_{X_d} X_d + \chi_{X_{\text{ac}}} X_{\text{ac}} + \chi_{Y_{\text{bc}}} Y_{\text{bc}} + \chi_{Y_d} Y_d \\ &+ \chi_{Y_{\text{ac}}} Y_{\text{ac}} + \chi_{X_{\text{bc}}} X_{\text{bc}}) / \chi_F \end{aligned}$$

The total power spectral density(PSD) is

$$\begin{aligned} S_{\text{FF}}(\omega) &= \int d\omega' \langle F(\omega) F(\omega') \rangle \quad (34) \\ &= S_{\text{FF}}^{\text{th}}(\omega) + S_{\text{FF}}^{\text{shot}}(\omega) \end{aligned}$$

where the thermal noise PSD is

$$\begin{aligned} S_{\text{FF}}^{\text{th}}(\omega) &= \int d\omega' \langle \xi(\omega) \xi(\omega') \rangle \quad (35) \\ &= 2m\gamma_m K_B T \end{aligned}$$

and the shot noise PSD is

$$\begin{aligned} S_{\text{FF}}^{\text{shot}}(\omega) &= \frac{1}{2} \left| \frac{\chi_{X_d} - i\chi_{Y_d}}{\chi_F} \right|^2 + \frac{1}{2} \left| \frac{\chi_{X_{\text{ac}}} - i\chi_{Y_{\text{ac}}}}{\chi_F} \right|^2 \quad (36) \\ &+ \frac{1}{2} \left| \frac{\chi_{X_{\text{bc}}} - i\chi_{Y_{\text{bc}}}}{\chi_F} \right|^2 \end{aligned}$$

For a Dc ( $\omega = 0$ ) force, we have

$$\left| \frac{\chi_{X_d} - i\chi_{Y_d}}{\chi_F} \right|^2 = \frac{\hbar m \omega_m^2 \kappa_{\text{ex}} (\kappa g_1 x_s)^2 g_2^2 + \frac{(g_2^4 - 3(\kappa g_1 x_s)^2)^2}{4g_2^2}}{2 \kappa (\kappa g_1 x_s)^3} \quad (37)$$

$$\left| \frac{\chi_{X_{\text{ac}}} - i\chi_{Y_{\text{ac}}}}{\chi_F} \right|^2 = \frac{\hbar m \omega_m^2 \kappa_a (\kappa g_1 x_s)^2 g_2^2 + \frac{9(\kappa g_1 x_s)^4}{g_2^2}}{2 \kappa (\kappa g_1 x_s)^3} \quad (38)$$

$$\left| \frac{\chi_{X_{\text{bc}}} - i\chi_{Y_{\text{bc}}}}{\chi_F} \right|^2 = \frac{\hbar m \omega_m^2 \kappa_b \kappa^2 g_2^4 + (g_1 x_s \kappa)^2}{2 \kappa (\kappa g_1 x_s)^3} \quad (39)$$

here we have assumed  $\kappa_a, \kappa_b \ll g_2, \kappa_{\text{ex}}$ . Then, the noise PSD becomes

$$S_{\text{FF}}^{\text{shot}}(0) \simeq \frac{\hbar m \omega_m^2}{4} \left[ \frac{1}{2} \frac{g_2^6}{(\kappa g_1 x_s)^3} - \frac{g_2^2}{(\kappa g_1 x_s)} + \frac{9}{2} \frac{(\kappa g_1 x_s)}{g_2^2} \right], \quad (40)$$

When  $g_2^2 \simeq 1.45\kappa g_1 x_s$  is satisfied, the power spectra density can be minimized

$$S_{\text{FF}}^{\text{shot}}(0) \simeq 0.8\hbar m \omega_m^2 \quad (41)$$

This is the square of the force detection sensitivity

---

[1] D. D. Smith, H. Chang, K. A. Fuller, A. T. Rosenberger, and R. W. Boyd, Phys. Rev. A **69**, 063804 (2004).

- [2] A. Naweed, G. Farca, S. I. Shopova, and A. T. Rosenberger, *Phys. Rev. A* **71**, 043804 (2005).
- [3] Q. Xu, S. Sandhu, M. L. Povinelli, J. Shakya, S. Fan, and M. Lipson, *Phys. Rev. Lett.* **96**, 123901 (2006).
- [4] K. Totsuka, N. Kobayashi, and M. Tomita, *Phys. Rev. Lett.* **98**, 213904 (2007).
- [5] Q. Xu, J. Shakya, and M. Lipson, *Opt. Express* **14**, 6463 (2006).
- [6] M. Mancinelli, R. Guider, P. Bettotti, M. Masi, M. R. Vanacharla, and L. Pavesi, *Opt. Express* **19**, 12227 (2011).
- [7] N. Liu, T. Weiss, M. Mesch, L. Langguth, U. Eigenthaler, M. Hirscher, C. Sönnichsen, and H. Giessen, *Nano Letters* **10**, 1103 (2009).
- [8] Y. Lu, L. Xu, M. Shu, P. Wang, and J. Yao, *Photonics Technology Letters IEEE* **20**, 529 (2008).
- [9] B. Maes, P. Bienstman, and R. Baets, *J. Opt. Soc. Am. B* **22**, 1778 (2005).
- [10] N. Ganapathisubramanian and K. Showalter, *The Journal of chemical physics* **80**, 4177 (1984).
- [11] W. Chen, D. Goldbaum, M. Bhattacharya, and P. Meystre, *Physical Review A* **81**, 053833 (2010).
- [12] D. Vitali, S. Mancini, and P. Tombesi, *Phys. Rev. A* **64**, 051401 (2001).
- [13] M. Lucamarini, D. Vitali, and P. Tombesi, *Phys. Rev. A* **74**, 063816 (2006).
- [14] J. D. Teufel, T. Donner, M. A. Castellanos-Beltran, J. W. Harlow, and K. W. Lehnert, *Nature Nanotechnology* **4**, 820 (2009).
- [15] E. Gavartin, P. Verlot, and T. Kippenberg, *Nature Nanotechnology* **7**, 509 (2012).
- [16] S. Weis, *Science* **330**, 1 (2010).
- [17] A. H. Safavi-Naeini, *Nature* **472**, 69 (2011).
- [18] L. Fan, K. Y. Fong, M. Poot, and H. X. Tang, *Nature Communications* **6**, 5850 (2015).
- [19] M. O. Scully and M. Fleischhauer, *Phys. Rev. Lett.* **69**, 1360 (1992).
- [20] H. Lee, M. Fleischhauer, and M. O. Scully, *Physical Review A* **58**, 2587 (1998).
- [21] A. K. Mohapatra, T. R. Jackson, and A. Cs., *Physical Review Letters* **98**, 113003 (2007).
- [22] J. Q. Zhang, Y. Li, M. Feng, and Y. Xu, *Phys. Rev. A* **86**, 10870 (2012).
- [23] J. Qi, F. C. Spano, T. Kirova, A. Lazoudis, J. Magnes, L. Li, L. M. Narducci, R. W. Field, and A. M. Lyyra, *Physical Review Letters* **88**, 173003 (2002).
- [24] I. S. Gradshteyn and I. M. Ryzhik, *New York Academic Press* **103** (1994).
- [25] Y.-q. Li and M. Xiao, *Phys. Rev. A* **51**, 4959 (1995).